Inter-node Distance Estimation from Ambient Acoustic Noise in Mobile Underwater Sensor Arrays

Riley Yeakle, Perry Naughton, and Ryan Kastner
Department of Computer Science and Engineering
University of California, San Diego
La Jolla, CA
Email: {ryeakle, pnaughto, kastner}@eng.ucsd.edu

Curt Schurgers
Qualcomm Institute, Calit2
University of California, San Diego
La Jolla, CA
Email: cschurgers@eng.ucsd.edu

***Abstract*—As the number of units in underwater sensor arrays grow, low-cost localization becomes increasingly important to maintain network scalability. Methods using ambient ocean noise are promising solutions because they do not require external infrastructure, nor expensive on-board sensors. Here we extend past work in stationary array element localization from correlations of ambient noise to a mobile sensor array [1]. After obtaining inter-node distance estimates using ambient noise correlations, these distances can be used to determine a relative localization of an array of mobile underwater sensor platforms without introducing any external infrastructure or on-board localization sensors.**

In this work we explore the effects of receiver mobility on inter-node distance estimation via correlations of ambient acoustic noise. Through analysis and simulation, we develop an exact solution along with a more tractable approximation to the peak amplitude of the Time-Domain Green's Function between the two mobile receivers, which provides an estimate of their spatial separation. Here we demonstrate that the mobile noise correlation amplitude at the time delay for a sound wave traveling from one receiver to the other can be modeled with the wideband ambiguity function of a single sound source. We then use this approximation to discuss selection of design parameters and their effects on the noise correlation function.

I. Introduction

Understanding the planet's oceans is key in understanding our planet's health. Ocean monitoring via sensor arrays can be challenging because of the difficulty of communicating with underwater sensor platforms. Beneath the surface, devices no longer have access to radio communications, including GPS which makes localization challenging.

In this work we will address the problem of estimating inter-node distances between the receiver pairs of a slowly moving underwater sensor array using only the ambient acoustic noise recorded at each unit. A set of pairwise distance estimates for all the nodes in our network is sufficient to come up with a relative localization for the array elements [1] [2]. This can then turn into a global localization solution if we know the absolute positions of a few 'anchor units'.

Past work in hydrophone localization shows that long term correlations of ambient noise recorded at two nearby stationary hydrophones can estimate the Time-Domain Green's Function (analogous to the impulse response in linear systems theory) between the two receivers [3]. In isotropic sound fields, this noise correlation function produces a peak at the time it takes for a sound wave to travel from one receiver to the other and thus can act as an estimator for the distance between the receiver pair. This function can be used to estimate the distance between our receivers by finding the times at which these two peaks occur, as shown in Figure 1. In terms of signal to noise ratio for this distance estimator, the average amplitude of the two impulses gives our signal strength while the standard deviation of the correlation noise outside of these peaks is our noise level. There are two key problems which arise as we extend this theory to the mobile receiver case: Doppler shift and non-stationarity.

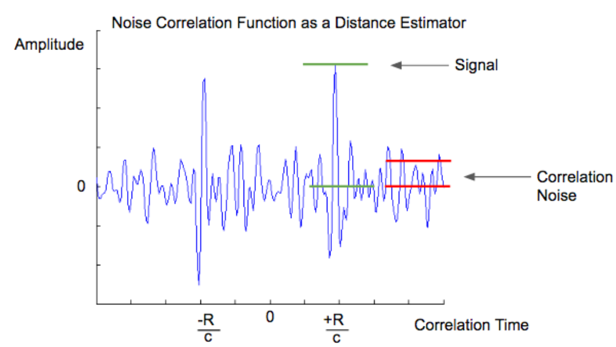

Fig. 1. Illustration of the ambient noise correlation function as a distance estimator. For this estimator, we choose the distance corresponding to the peaks amplitude of this function in either positive or negative correlation time. Not to be confused with the ambient noise sources, the noise in this estimator is the correlation noise level found beyond the two time-symmetric peaks.

In the mobile case, the recorded signal at each receiver undergoes a Doppler shift determined by the receiver's relative velocity with respect to each of the individual sources. For a single source, the wideband ambiguity function, describes the correlation amplitude of a Doppler shifted and delayed signal with itself [4]. However, it remains to show how this relates to the correlation of an entire field of sources on the emergence of the Time-Domain Green's Function. Next, we have the complication of non-stationarity during the correlation window. In the stationary receiver case, the SNR of the noise correlation function as a distance estimator increases with increasing correlation time windows [5]. When the receivers are mobile the longer the correlation window, the approximation of the system as roughly stationary becomes worse and eventually may destroy the peaks of the noise correlation function. Thus, in choosing our correlation time window, we need to pick a time window which is both long enough for the noise correlation peaks to emerge, but short enough that the receivers don't move too much during correlation.

To solve this problem, we will begin by examining the emergence of the Time-Domain Green's Function from correlations of ambient noise to see which components of the process will carry to the mobile receiver case. Next we will directly apply the wideband ambiguity function to the noise correlation function to provide an exact solution to the expected value of the noise correlation function's peak amplitudes, assuming one knew everything about the ambient noise sources in the environment and their spatial distribution. Since the exact solution requires immense knowledge about the ambient sound environment, we will then develop a practical approximation to the noise correlation function's peak amplitude as a function of the stationary noise correlation function and the wideband ambiguity function of a single source. Finally, we will use this approximation to formulate an objective function for optimizing the SNR of the noise correlation function distance estimator which can be used to choose the optimal correlation time window and determine maximum mobility conditions for a given SNR requirement.

The contributions of this paper are:

- An exact solution to the expected value of the noise correlation function peak amplitude between two receivers moving with constant velocity
- A first order approximation of the peak amplitude of the noise correlation function using the noise correlation function's peak amplitude in the stationary receiver case and the wideband ambiguity function for a single noise source
- An objective function for optimizing the SNR of the NCF distance estimator which can be used to choose the optimal correlation window length and determine maximum mobility conditions for a given SNR requirement

II. Background

A. Distance Estimation via Ambient Noise

The key result we build on is the emergence of an estimate of the Time-Domain Green's Function from correlations of ambient acoustic noise between two hydrophones [3] [6]. The Time-Domain Green's Function describes the propagation of a wave from one point in space to another and is analogous to the impulse response used in linear systems theory. In the context of sensor arrays, the Time-Domain Green's Function (now referred to as TDGF) between two receivers tells us how a source will propagate from one receiver to the other. We will first consider the system shown in Figure 2 in which two receivers record sound sources originating from different locations indicated with triangles over some time window T. For a system with a single direct path between two receivers, the TDGF will look like two symmetric impulses at $\pm\frac{R}{c}$ where R is the distance between the two array elements and c is the speed of sound. If we know c, we can then estimate the distance between the two receivers. Here we present an intuitive explanation for the emergence of the TDGF from ambient acoustic noise correlations which will be important to understanding how receiver motion during correlation will affect the emergence of correlation peaks at $\pm\frac{R}{c}$.

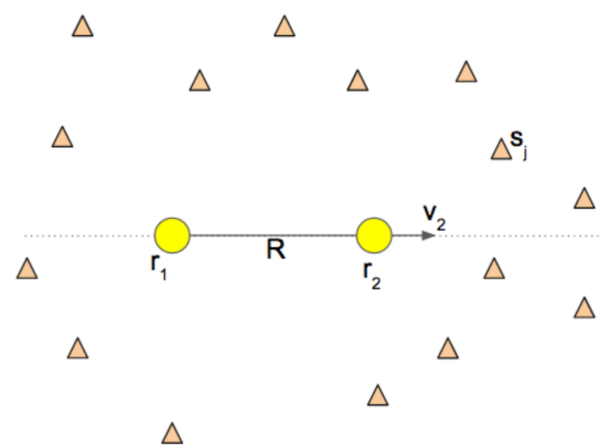

Fig. 2. Example of receiver and source setup in a 2D plane. Sources s_1 to s_j are distributed around the receiver pair and represent active sources at this instant in time. Receivers r_1 and r_2 are separated by a distance R and each have velocity v_i along the axis passing through the pair.

The first insight in developing the theory of ambient noise correlation is that the cross correlation function has a well-defined directivity pattern, meaning *it is sensitive to sources originating from certain directions more than others*. To see this, consider the scenario pictured in 2. The time delay produced by a single distant source under cross correlation is given as a function of angle of approach θ_0 (defined with respect to the axis between our receiver pair):

$$\tau_s = \frac{R}{c}\cos(\theta_0) \tag{1}$$

Since $cos(\theta_0)$ changes slowly near $\theta_0 = 0$ and $\theta_0 = \pi$, we expect sources with angle of approach near the axis of the receivers ($\theta_0 \approx 0$ and $\theta_0 \approx \pi$) to produce delay estimates closer in time to each other than those off the axis through the receivers. Consequentially, we expect larger correlation peaks to build up near τ_s corresponding to $\theta_0 \approx 0$ or π than anywhere else. Specifically, this τ_s is $\pm\frac{R}{c}$ gives the time of flight from one receiver to the other. As demonstrated in [6], the relative proportion of sources contributing to the correlation peak at $\tau = \pm\frac{R}{c}$ can be modeled using the directivity of the correlation function. Using this, the authors in [6] show that the ratio of 'coherent' sources (sources contributing to a correlation peak at $\tau = \pm\frac{R}{c}$), versus 'incoherent' sources (those contributing to correlation peaks elsewhere) can be expressed as:

$$Ratio(\theta_0) = \sqrt{\frac{2\pi f_c}{c} R} \left(1 + \frac{1}{12}\left(\frac{B}{f_c}\right)^2\right)^{\frac{1}{4}} \sin(\theta_0) \qquad (2)$$

where θ_0 is the angle of approach. In an isotropic sound field (meaning uniformly distributed source locations), the number of coherent sources is far greater than any θ_0 corresponding to a different time difference of arrival. Thus by correlating over long time windows the noise correlation function produces roughly symmetric peaks at $\tau = \pm\frac{R}{c}$.

Borrowing vocabulary from [6] and [1], we use the term 'endfire' to refer to the region around $\theta \in \{0, \pi\}$ for which sound sources make a significant contribution to the correlation peaks at $\tau = \pm\frac{R}{c}$. We can define this region more specifically using the directivity of the cross correlation function between our receivers and choosing the angle $\theta_{endfire}$ to be the effective beamwidth of the beam centered on $\theta = 0$ or equivalently $\theta = \pi$.

To get the cleanest correlation results, this technique uses the preprocessing pipeline shown in Figure 3 to compute the noise correlation function, which consists of bandpass and whitening steps. The bandpass step gives us control over what sorts of ambient sounds we look at, while the whitening step mitigates the effects of strong frequencies on the correlation. After preprocessing, we compute the noise correlation function using:

$$C_{y_1,y_2}(\tau) = \frac{1}{T}\int_{-T/2}^{T/2} y_1(t) y_2(t-\tau) dt \qquad (3)$$

$$NCF(\tau) = \frac{C_{y_1,y_2}(\tau)}{\frac{1}{T}\sqrt{\left(\int_{-T/2}^{T/2} y_1^2(t)dt\right)\left(\int_{-T/2}^{T/2} y_2^2(t-\tau)dt\right)}} \qquad (4)$$

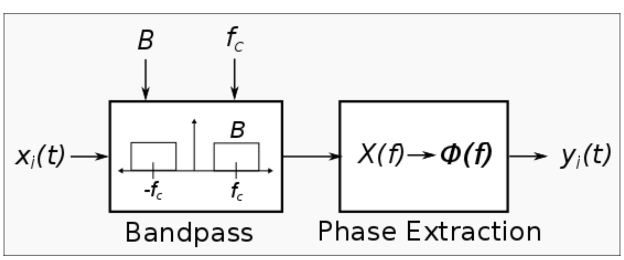

Fig. 3. Preprocessing pipeline used to compute the noise correlation function. The bandpass step allows us to focus on a specific noise frequency band, and the whitening step prevents the correlation from being biased by dominant frequency components.

B. The Wideband Ambiguity Function

For a single source, the problem of the correlation of a Doppler shifted signal across two receivers is modeled by the wideband ambiguity function, originally developed for studying radar responses to high velocity targets using broad spectrum radar pulses [4]. The ambiguity function describes the matched filter response of a delayed and Doppler mismatched pulse with the original signal. In computing the noise correlation function over a single source, we are essentially running a matched filter across our receivers and thus the wideband ambiguity function describes how our correlation will behave with receiver velocity and delay errors. As shown in [4] for a single source s, the wideband ambiguity function for cross correlation can be written as:

$$A(\tau, \beta) = \int s(t) s^*(\beta(t+\tau)) dt \qquad (5)$$

In particular we will be interested in the normalized version of this function for a broadband, flat spectrum, Gaussian signal. Normalized in this case meaning we want to know the correlation coefficient between the original signal and the Doppler shifted and delayed signal. In [7] the authors compute the normalized ambiguity function for just that signal and find the following:

$$\rho(\gamma = 0, \dot{\mu}) = \frac{1}{2b}\left[Si((a+1)b) - Si((a-1)b)\right] \qquad (6)$$

with:

$$Si(x) = \int_0^x \frac{\sin x}{x} dx$$

and $a = \frac{2}{f_c}$, and $b = \frac{\pi}{2}(B\dot{\mu}T)$, where f_c denotes the center frequency of our signal, B denotes its one-sided bandwidth, and T denotes the length of our correlation window, γ indicates the delay error, and $\dot{\mu}$ denotes the rate of change for the time delay between our two receivers. For a single mobile receiver, $\dot{\mu} = \frac{v_{rel}}{c}$ and for two mobile receivers it is given as $\frac{1+\frac{v_2}{c}\cos(\theta_2)}{1+\frac{v_1}{c}\cos(\theta_1)} - 1$.

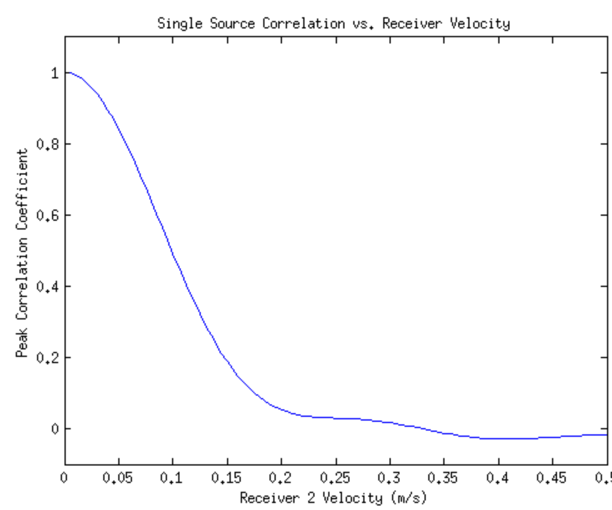

Fig. 4. Example of a zero time delay error cut of the normalized ambiguity function for a broadband, flat spectrum, Gaussian pulse.

This function represents the zero delay error cut of the ambiguity function of the matched filter over two receivers, which describes the correlation peak as a function at time delay $\tau = \frac{R}{c}$, corresponding with the separation of the receivers at time 0 (halfway through the correlation), and relative Doppler shift across each receiver $\dot{\mu}$.

III. Problem Formulation

We make the following simplifying assumptions to develop our theory on the effects of receiver mobility during noise correlation:

- Our sources are stationary in space, transient in time, and generated from uncorrelated Gaussian processes with mean 0 and variance σ_s^2
- Our sources have a spectrum extending beyond the bandwidth over which we correlate
- All sources propagate in a single direct path from source to receiver
- In correlation preprocessing, we use $f_{min} \geq 100Hz$
- There are a large number of sound events over our correlation time window
- Our receiver velocity is significantly less than the speed of sound in the medium and is taken with respect to the axis through the receivers

These assumptions form the simplest case for describing the effect of receiver motion on the noise correlation function. Our assumption of correlation bandwidth smaller than the noise bandwidth is reasonable so long as we choose our bandwidth and center frequency in a manner consistent with the actual spectrum of ambient ocean noise. The constraint of $f_{min} \geq 100Hz$ ensures that our correlation directivity intuition holds since low frequencies exhibit much less directivity than higher frequencies for a pair of omnidirectional receivers.

We choose to take the receiver velocity along the axis because in a relatively uniform spatial distribution of short sound events, the relevant velocity term is how much the receivers move with respect to each other since the sound field looks the same in all directions. In a more directional sound field, the rotation of the receivers would be important because it would affect the distribution of sources in the endfire regions over time. However, strongly directional sound fields tend to distort the emergence of the Time-Domain Green's Function from correlations of ambient noise, so this method is unsuitable for those environments.

IV. Exact Solution

Here we build on the previous section to relate the normalized ambiguity function for a single source $\rho(\gamma = 0, \dot{\mu})$ to the noise correlation function at time $\tau = \pm\frac{R}{c}$ in the presence of constant receiver velocity.

In a field of j sound sources, we can write the signal received at receiver i as:

$$x_i(t) = \sum_{j=1}^{N} \alpha_{i,j} s_j((\beta_{i,j}(t + \mu_{i,j}) + D_j) \tag{7}$$

where $\alpha_{i,j}$ is the attenuation between source j and receiver i, $\beta_{i,j}$ is the time scaling between source i and receiver j (with $\beta_{i,j} = (1 + \frac{v_i}{c}\cos(\theta_{i,j}))$, $\mu_{i,j}$ is the time delay for the source traveling to the receiver at the start of correlation, and D_j is the start time of source j.

Next, we define the following:

$$\hat{\sigma}_y = \sqrt{\int_{-\frac{T}{2}}^{\frac{T}{2}} y^2(t)dt} \tag{8}$$

as the square root of the energy of a signal $y(t)$.

Next, we have the correlation coefficient $\rho_{y_1,y_2}(\tau)$ given by:

$$\rho_{y_1,y_2}(\tau) = \frac{1}{\hat{\sigma}_{y_1}\hat{\sigma}_{y_2}}\left(\frac{1}{T}\int_{-\frac{T}{2}}^{\frac{T}{2}} y_1(t)y_2(t-\tau)dt\right) \tag{9}$$

Finally, let $y'(t)$ be the ideal bandpass filtered version of $y(t)$, as performed in the noise correlation pre-processing step before whitening. We can then relate the noise correlation function to the velocity correlation coefficients for each individual source in our field as follows:

$$NCF_{x_1,x_2}(\tau, t, v_1, v_2) = \rho_{x_1',x_2'}(\tau) \tag{10}$$

$$= \frac{1}{\hat{\sigma}_{x_1'}\hat{\sigma}_{x_2'}}\frac{1}{T}\int_{-\frac{T}{2}}^{\frac{T}{2}} x_1'(t)x_2'(t-\tau)dt \tag{11}$$

Then, since we assume uncorrelated sources, the cross terms in the product $x_1'(t)x_2'(t-\tau)$ cancel and we are left with:

$$\frac{1}{\hat{\sigma}_{x_1'}\hat{\sigma}_{x_2'}}\sum_{j=1}^{N}\alpha_{1,j}\alpha_{2,j}\frac{1}{T}\int_{-\frac{T}{2}}^{\frac{T}{2}} s_{1,j}'(t)s_{2,j}'(t-\tau)dt \tag{12}$$

Since $s_{1,j}'$ and $s_{2,j}'$ are related as time scaled and shifted versions of each other, we can replace the integral with their normalized ambiguity function to obtain:

$$\frac{1}{\hat{\sigma}_{x_1'}\hat{\sigma}_{x_2'}}\sum_{j=1}^{N}\alpha_{1,j}\alpha_{2,j}\hat{\sigma}_{s_{1,j}'}\hat{\sigma}_{s_{2,j}'}\rho_{s_{1,j}',s_{2,j}'}(\tau, \dot{\mu}_j) \tag{13}$$

After further simplification and reduction taking advantage of our flat, bandpass power spectrum after preprocessing, we obtain:

$$NCF(\tau, t, v_1, v_2) = \frac{\sum_{j=1}^{N}\alpha_{1,j}\alpha_{2,j}\hat{\sigma}_{s_{1,j}'}\hat{\sigma}_{s_{2,j}'}\rho_{s_{1,j}',s_{2,j}'}(\tau, \dot{\mu}_j)}{N\sigma_{s'}^2\sqrt{E\left[\frac{\alpha_{1,j}^2}{\beta_{1,j}^2}\right]E\left[\frac{\alpha_{2,j}^2}{\beta_{2,j}^2}\right]}} \tag{14}$$

Noting that the numerator converges to its expected value for large N as well, we finally obtain:

$$NCF(\tau, t, v_1, v_2) = \frac{E\left[\alpha_{1,j}\alpha_{2,j}\hat{\sigma}_{s_{1,j}'}\hat{\sigma}_{s_{2,j}'}\rho_{s_{1,j}',s_{2,j}'}(\tau, \dot{\mu}_j)\right]}{\sigma_{s'}^2\sqrt{E\left[\frac{\alpha_{1,j}^2}{\beta_{1,j}^2}\right]E\left[\frac{\alpha_{2,j}^2}{\beta_{2,j}^2}\right]}} \tag{15}$$

$$= \frac{E\left[\frac{\alpha_{1,j}}{\beta_{1,j}}\frac{\alpha_{2,j}}{\beta_{2,j}}\rho_{s_{1,j}',s_{2,j}'}(\tau, \dot{\mu}_j)\right]}{\sqrt{E\left[\frac{\alpha_{1,j}^2}{\beta_{1,j}^2}\right]E\left[\frac{\alpha_{2,j}^2}{\beta_{2,j}^2}\right]}} \tag{16}$$

V. Developing a Useful Approximation

While Equation 15 gives us an exact expression for the noise correlation function between two moving receivers in a sound field with a known distribution, it is not particularly insightful in this form. Here we develop an approximation relating the noise correlation function amplitude at the receiver separation at time $t = 0$ as a function of velocity to the correlation coefficient of a single source across the two receivers.

A. Behavior of Endfire Sources

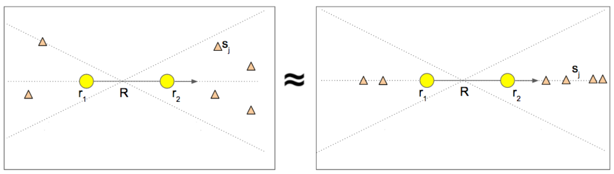

Fig. 5. Virtual source argument in pictures demonstrates how we can represent a set of sources in the endfire region as a single virtual source. We begin with a set of sources in the endfire region. Due to the small angle of sources in the endfire region, we can nudge off-axis sources onto the axis through the receivers with approximately the same effect on the receivers. Now that the receiver velocity with respect to all these sources is the same we can replace the sources with a single virtual source with a time series equivalent to the sum of the axis sources. After noise correlation preprocessing, this virtual source captures the net effect of all the endfire sources.

We first note that only sources inside the endfire beam will make significant contributions to the noise correlation function. Sources outside this beam do not make a meaningful contribution to the noise correlation peak at $\tau = +\frac{R}{c}$ (which we will refer to as τ^+).

Note that the net effect of these sources as heard by receiver i can be written as:

$$x_i(t) = \sum_{j \in E^+} \alpha_{i,j} s_j(\beta_{i,j}(t + D_{i,j})) \tag{17}$$

where E^+ denotes the set of sources in the endfire beam corresponding to τ^+.

The key insight in developing our approximation is that these sources in a given endfire beam collectively can be approximated with a single source. Recall that $\beta_{i,j} = 1 + \frac{v_i}{c}\cos(\theta_{i,j})$ and that in an endfire beam, $\cos(\theta_{i,j})$ is near 1 for all sources and both receivers. Thus, we can approximate $\beta_{i,j}$ in the endfire region using this small angle approximation for cosine as $\beta_{i,j} \approx 1 + \frac{v_i}{c}$, removing the dependence on θ for the velocity term. Physically, this approximation is equivalent to nudging all endfire sources onto the axis passing through the receivers. This new process behaves like a single source on the axis passing through the receivers since the received signal $x(t)$ is the same if we replace the set of sources now on the axis with a single source equal to a linear combination of the individual sources on the axis. Since we assume the original sources are all Gaussian, this virtual source is as well.

Finally, to demonstrate the applicability of the Gaussian matched filter wideband ambiguity function to the model, we show that after pre-filtering, the virtual source produces a pre-correlation term with flat power spectrum over a given bandwidth. For a single source with receiver motion, in the frequency domain we get the following:

$$S_{i,j}(f) = \left|\frac{1}{\beta_{i,j}}\right| S_j\left(\frac{f}{\beta_{i,j}}\right) e^{-j2\pi f D_{i,j}\beta_{i,j}} \tag{18}$$

From 18 we can see that the receiver motion either expands or contracts the original source spectrum by a relatively small amount since for low receiver velocity $\beta_{i,j} \approx 1$ since we assume that $\frac{v_i}{c} \ll 1$. By linearity of the Fourier transform, we can then see that the received signal spectrum for a set of sources will be a slightly dilated version of the original spectrum. After bandpassing out our frequencies of interest and whitening via extracting the Fourier transform phase, we're left with spectral properties matching what we would see in the stationary case. Therefore we can approximate the set of sources in the endfire beam during the correlation window as a single virtual source. The mobile noise correlation function for this virtual source is then given by the normalized wideband ambiguity function for a broadband, flat spectrum source. Next, we relate this approximation back to the full field noise correlation in which we have sources both inside and outside the endfire beams.

B. Relationship to Stationary Noise Correlation Function

Under this virtual source argument, we are approximating the net effect of all our endfire sources with a single source on the axis through the receiver pair. We now need to show what happens to this function when we include the noise from sound sources outside the endfire beam. Combining this approximation for the sources in our endfire beam with the exact solution presented in equation 15 we get:

$$NCF(\tau^+, v_1, v_2) \approx \frac{\sum_{j \in E^+} \left[\frac{\alpha_{1,j}}{\beta_{1,j}} \frac{\alpha_{2,j}}{\beta_{2,j}}\right]}{N\sqrt{E\left[\frac{\alpha_{1,j}^2}{\beta_{1,j}^2}\right] E\left[\frac{\alpha_{2,j}^2}{\beta_{2,j}^2}\right]}} \rho(0, \dot{\mu}_{axis}) \tag{19}$$

The term in front of the normalized ambiguity function cut $\rho(0, \dot{\mu}_{axis})$ can be approximated as a constant A. Since we assume $\frac{v}{c} \ll 1$, we have $\beta_{i,j} \approx 1$ and thus this front term is approximately constant. We know at zero velocity this approximation should be equal to the exact expression for the noise correlation function over the given distribution of sound sources. Since $\rho(0, 0) = 1$ for our virtual source, we have:

$$A = NCF(\tau^+, v_1 = 0, v_2 = 0) \tag{20}$$

Thus we can approximate the noise correlation function as:

$$NCF(\tau^+, v_1, v_2) \approx NCF(\tau^+, 0, 0)\rho(0, \dot{\mu}_{axis}) \tag{21}$$

which holds as long as our low velocity assumption is correct.

The proposed approximation does two important things. First, it decouples the effects of receiver velocity from the actual distribution of sound sources in our environment. Second, it shows the behavior of the noise correlation function at our time of interest looks like a scaled version of the behavior of a single source on the axis passing through the receivers.

VI. SIMULATIONS

To confirm the proposed hypotheses on the noise correlation function's behavior under receiver velocity given our assumptions, we present simulation which show that our proposed first order approximation holds.

A. Simulation Setup

Each simulation scenario begins with picking a distribution of sound sources and a set of paths for each receiver. We select the start and end position of each receiver for each velocity such that halfway through the correlation the receivers are the same distance apart. This ensures that we always have the same separation at $t = 0$ regardless of the receiver velocity.

Sources are generated using independent bandpassed standard normal processes for a duration of 0.1 seconds. The spatial distribution of sources varies from experiment to experiment, however the distribution of start times is distributed uniformly over the experiment time window in all cases.

To propagate the sources to each receiver, we use the model in which the signal received is given by:

$$s_{i,j}(t) = \left(\frac{1}{1+d}\right) s_j\left(\left(1 + \frac{v_{rel}}{c}\right)(t + D)\right) \quad (22)$$

which corresponds with our receiver having a constant velocity with respect to the source (reasonable since our sources are short in duration and our receivers move slowly) and attenuation due to spherical spreading $\approx \frac{1}{d}$ where d is the distance from source to receiver (corresponding with a $\frac{1}{d^2}$ dropoff in signal energy). The $\frac{1}{1+d}$ attenuation factor ensures that a source at 0 distance from our receiver experiences no attenuation and corresponds with a source origin power of $\sigma_s^2 = 1$.

Holding the source distribution constant, we generate audio as heard by each receiver for a set of constant velocities. We then repeat the experiment with a new realization of the source positions and start times for a set number of trials depending on the variance inherent in the distribution. For example, results from isotropic distributions tend to be noisier than those with sources only in the endfire beams, so we perform more trials on the isotropic distributions in order to increase the certainty of our results.

In simulation we explore the following source distributions:

1) Sources on the axis passing through the receiver pair
2) Sources distributed in the $2D$ endfire regions of the receiver pair
3) Sources distributed isotropically over the $2D$ plane containing the receivers
4) Receivers at constant $10m$ depth, sources distributed isotropically in a 2D plane at the surface

Case 1 serves as a verification of our intuition that sources on the axis behave like a single virtual source on each side of the receiver pair. Case 2 serves to demonstrate that our proposed approximation holds for sources in the endfire beams of the receivers. Cases 3 and 4 demonstrate the most realistic cases in which we test to see how well our approximation holds in isotropic sound field cases. Case 4 is a more realistic case of source distribution, more closely representing surface noise seen in practice [8].

After computing the empirical noise correlation function values for each value in each trial, we compute the mean and standard deviation of the estimates which we use to form 90% confidence intervals for the average noise correlation amplitude of each receiver pair velocity across our set of source distribution realizations. This gives us a relative sense of certainty about these empirical estimates.

These simulations are intended to demonstrate that our model does indeed reflect the behavior of the noise correlation function in a simple environment.

B. Simulation Results

First, we confirm our previous argument that the noise correlation function of a set of sources along the axis passing the receivers is well modeled by the ambiguity function of a single source on the axis.

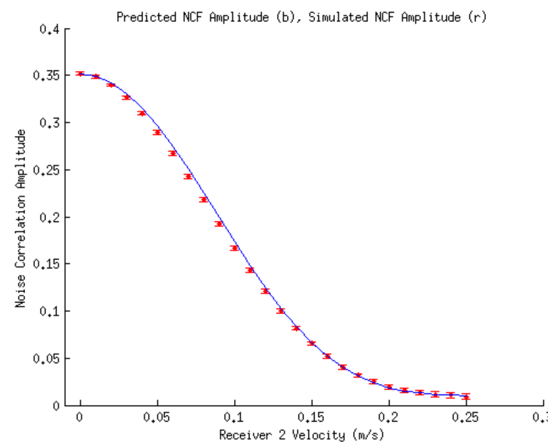

Fig. 6. Predicted and simulated correlation coefficients for a single receiver moving, with all sources distributed uniformly along the axis between the two receivers. The y axis is the noise correlation function amplitude at τ^+ and the x axis is the velocity of receiver 2. Red indicates simulated values along with 90% confidence intervals and blue is the predicted quantity: $NCF(\tau^+, 0, 0)\rho(0, \dot{\mu}_{axis})$. Overall we see a close match between simulated and predicted values. This confirms our intuition that many sources along the axis between the receivers behaves like a single source.

Figure 6 demonstrates that as predicted, sources on the axis passing through our receiver pair can be modeled with a pair of virtual sources, one for each endfire beam of our receiver pair. Note that our peak value for the correlation is not equal to 0.5 for sources along the axis, due to the correlation preprocessing and sources between the two receivers contributing to peaks not at $\tau = \tau^+$ or $\tau = \tau^-$.

Next, we demonstrate that a field composed of only sources in the endfire beams is approximated by the ambiguity function for a single virtual source on the axis passing through the receivers.

Though not as good an approximation as the axis case, here we can see that our approximation holds reasonably well. In this case, the approximation tends to underbound the experimental bounds by a narrow margin. In the higher center

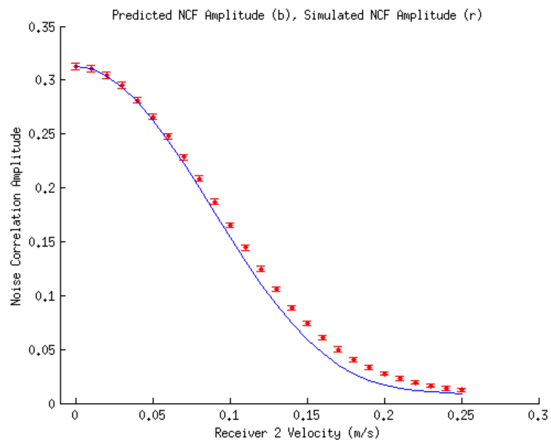

Fig. 7. Simulated and predicted noise correlation amplitude for varying velocities with sources distributed in the endfire regions of the receivers. The y axis is the noise correlation function amplitude at τ^+ and the x axis is the velocity of receiver 2. Red indicates simulated values along with 90% confidence intervals and blue is the predicted quantity: $NCF(\tau^+, 0, 0)\rho(0, \dot{\mu}_{axis})$. Like the axis case in Figure 6, the predicted values match the simulated values for low velocity, but tend to underbound the simulated values for larger velocities. This demonstrates that the approximation of sources in the endfire region as all being on the axis holds reasonably well.

frequency and bandwidth cases, the peak noise correlation value drops off much faster as a function of receiver velocity, but the approximation holds much more tightly because of the narrower endfire beamwidth in these cases.

In the cases with isotropically distributed noise, we start to see some interesting effects. Our approximation holds reasonably well for different bandwidths and center frequencies (Figures 8, and 9).

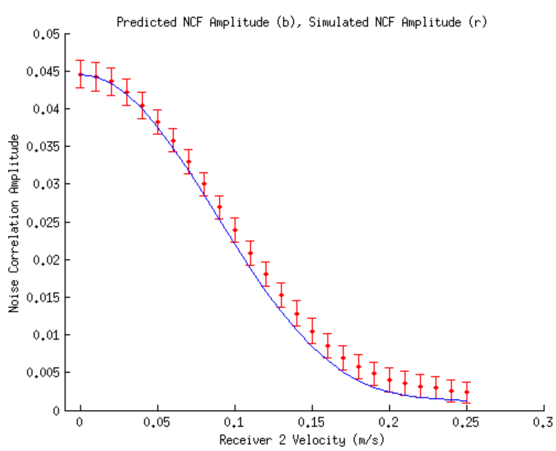

Fig. 8. Simulated and predicted noise correlation amplitude for varying velocities with sources distributed isotropically in the $2D$ plane of the receivers, $B = 400$, $f_c = 300$. The y axis is the noise correlation function amplitude at τ^+ and the x axis is the velocity of receiver 2. Red indicates simulated values along with 90% confidence intervals and blue is the predicted quantity: $NCF(\tau^+, 0, 0)\rho(0, \dot{\mu}_{axis})$. As predicted, the isotropic field case shown here is close in behavior to the endfire case in Figure 7. This demonstrates that the proposed approximation holds in the case of an isotropic field of sound sources.

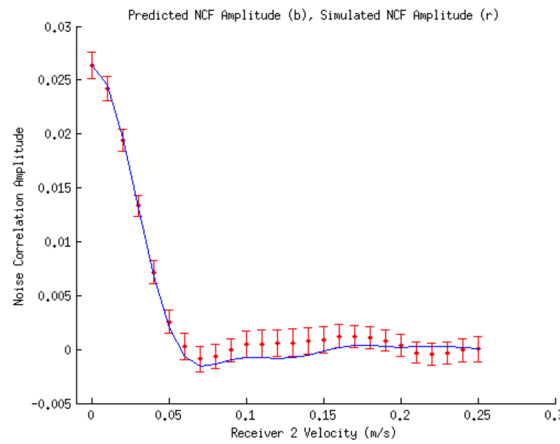

Fig. 9. Simulated and predicted noise correlation amplitude for varying velocities with sources distributed isotropically in the $2D$ plane of the receivers, $B = f_c = 1000$. The y axis is the noise correlation function amplitude at τ^+ and the x axis is the velocity of receiver 2. Red indicates simulated values along with 90% confidence intervals and blue is the predicted quantity: $NCF(\tau^+, 0, 0)\rho(0, \dot{\mu}_{axis})$. Similar to Figure 8 the prediction matches the simulation well. This shows that the proposed approximation also holds for different center frequencies and bandwidths.

Finally, we get to the most realistic case of sources residing in a plane above the receivers, corresponding with surface noise above receivers at constant depth. Like the previous two cases, we see that our predicted noise correlation value tends to underbound the experimental data by a small margin. This is acceptable from a design perspective because it allows us to choose our correlation parameters such that we will achieve slightly better than predicted performance. Similar to the 2D case we see that our approximation works well in the surface noise case (Figures 10).

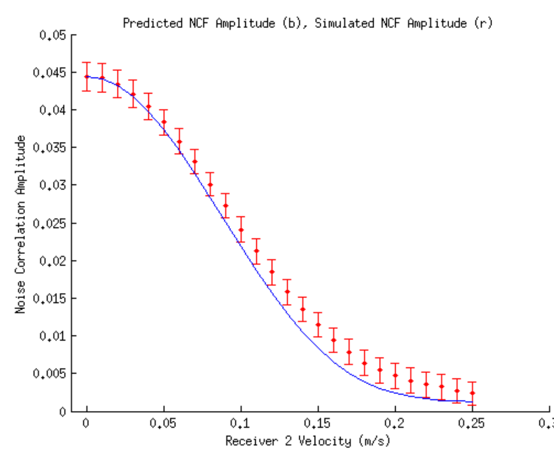

Fig. 10. Simulated and predicted noise correlation amplitude for varying velocities with sources distributed isotropically on the surface plane 10m above the receivers, $B = 400$, $f_c = 300$. The y axis is the noise correlation function amplitude at τ^+ and the x axis is the velocity of receiver 2. Red indicates simulated values along with 90% confidence intervals and blue is the predicted quantity: $NCF(\tau^+, 0, 0)\rho(0, \dot{\mu}_{axis})$. In this more realistic noise distribution case, the behavior similar to that in Figure 8 shows that this approximation holds for this surface noise distribution as well.

VII. Noise Correlation SNR

From previous work in ambient noise correlation [5], we know the signal to noise ratio of the amplitude of the TDGF peak to the correlation noise level is proportional to:

$$SNR \propto \left(\frac{\sqrt{BT}}{\sqrt{f_c}} \right) \tag{23}$$

Applying the mobile case approximation from Equation 21 ($NCF(\tau^+, v_1, v_2) \approx NCF(\tau^+, 0, 0)\rho(0, \dot{\mu})$) in the mobile case to this SNR expression, we get:

$$SNR \propto \left(\frac{\sqrt{BT}}{\sqrt{f_c}} \right) \rho(v_{axis}, B, T, f_c) \tag{24}$$

After combining with the wideband ambiguity function given in 6, we find that the signal to noise ratio is no longer monotonically increasing with increased correlation time and bandwidth. In terms of optimization, this provides us with an objective we can maximize over to get the best possible signal to noise ratio for given conditions. While the optimization for this is fairly straightforward (since one can quickly compute the objective over a large set of parameter values), there are two interesting problems this objective can address: optimal time window selection and maximum mobility conditions.

To find the optimal time window for a given receiver velocity, one can simply maximize Equation 24 over T. For determining the maximum tolerable velocity, one can choose a maximum attenuation α for the stationary case (*i.e.* the mobile amplitude must be at least α times the stationary case amplitude), represented by $\rho(v_{axis}, B, T, f_c)$. Then, after finding the minimum time window T_{min} required for the noise correlation function to emerge, one can find the maximum velocity the system can tolerate such that $T > T_{min}$ and $\rho(v_{axis}, B, T, f_c) >= \alpha$.

VIII. Conclusion

In exploring the effects of receiver mobility on inter-node distance estimation via correlations of ambient noise we've demonstrated that we can model the mobile noise correlation problem using the wideband ambiguity function. By approximating the set of noise sources in the endfire beams of our receiver pair as a single virtual source, we can reduce the problem of finding the noise correlation function of a mobile receiver pair to solving the normalized wideband ambiguity function of a single source on the axis through the receivers. Through simulation over common sound source distributions we've shown that with appropriate scaling this approximation predicts the amplitude of the mobile noise correlation function reasonably well, typically underbounding the simulated values by a small margin. We then demonstrated how this approximation can be combined with past work on the SNR of the noise correlation function to form an objective function for optimizing the SNR of the noise correlation function as a distance estimator in the mobile case, which can be used to select correlation time window and determine maximum mobility conditions for applying this method to inter-node distance estimation.

Acknowledgment

We'd like to thank the NSF for their support of this work under the grant CNS - 1344291 INSPIRE Track I: "Distributed Sensing Collective to Capture 3D Soundscapes" The authors would also like to thank Prof. William Hodgkiss for discussions which helped get this research started.

References

[1] K. G. Sabra, P. Roux, A. M. Thode, G. L. D'Spain, W. Hodgkiss, and W. Kuperman, "Using ocean ambient noise for array self-localization and self-synchronization," *Oceanic Engineering, IEEE Journal of*, vol. 30, no. 2, pp. 338–347, 2005.

[2] X. Ji and H. Zha, "Sensor positioning in wireless ad-hoc sensor networks using multidimensional scaling," in *INFOCOM 2004. Twenty-third AnnualJoint Conference of the IEEE Computer and Communications Societies*, vol. 4. IEEE, 2004, pp. 2652–2661.

[3] P. Roux and M. Fink, "Greens function estimation using secondary sources in a shallow water environment," *The Journal of the Acoustical Society of America*, vol. 113, no. 3, pp. 1406–1416, 2003.

[4] E. Kelly and R. Wishner, "Matched-filter theory for high-velocity, accelerating targets," *Military Electronics, IEEE Transactions on*, vol. 9, no. 1, pp. 56–69, 1965.

[5] K. G. Sabra, P. Roux, and W. A. Kuperman, "Emergence rate of the time-domain greens function from the ambient noise cross-correlation function," *The Journal of the Acoustical Society of America*, vol. 118, no. 6, pp. 3524–3531, 2005. [Online]. Available: http://scitation.aip.org/content/asa/journal/jasa/118/6/10.1121/1.2109059

[6] P. Roux, W. Kuperman, N. Group *et al.*, "Extracting coherent wave fronts from acoustic ambient noise in the ocean," *The Journal of the Acoustical Society of America*, vol. 116, no. 4, pp. 1995–2003, 2004.

[7] G. Johnson, D. Ohlms, and H. Hampton, "Broadband correlation processing," in *Acoustics, Speech, and Signal Processing, IEEE International Conference on ICASSP'83.*, vol. 8. IEEE, 1983, pp. 583–586.

[8] G. M. Wenz, "Acoustic ambient noise in the ocean: spectra and sources," *The Journal of the Acoustical Society of America*, vol. 34, no. 12, pp. 1936–1956, 1962.